SAND 88-7067C CONF-890855--31

ROBABILISTIC ESTIMATE OF SEISMIC DAMAGE TO THE WASTE-HANDLING BUILDING OF A REPOSITORY LOCATED AT YUCCA MOUNTAIN, NEVADA

O. K. Kiciman and N. A. Abrahamson

Bechtel National, Inc.
San Francisco, California 94119

SAND--88-7067C

DE89 011396

1.0 SCOPE

The waste-handling building (WHB) at the Yucca Mountain repository is a reinforced concrete structure with massive shear walls whose thicknesses are established by shielding requirements. The probabilities of seismic damage to the WHB are calculated in this paper. To determine these probabilities, seismic hazard curves for the site and fragility curves for the building were developed and combined. The details of this work are found in SNL (1988).

2.0 SEISMIC HAZARD

The seismic hazard analysis considers both ground acceleration at the WHB site and vertical ground rupture under the WHB. Standard methods (McGuire, 1976; 1978) were used to estimate the acceleration hazard assuming that there is no ground rupture under the WHB. The ground rupture hazard from unknown faults was estimated using a conservative approach developed in this study. The acceleration hazard associated with ground rupture under the WHB was also computed.

2.1 Acceleration Hazard

The faults in the Yucca Mountain region regarded as active for this study are shown in Figure 1. The base case activity rates of the faults and background seismicity were taken from URS/Blume (1987). These parameters were used to generate the base case acceleration hazard curve.

The uncertainty of the seismic hazard was estimated by varying significant model input parameters. To estimate the acceleration hazard, the following parameters were varied: attenuation model, slip model,

This work was supported by the U. S. Department of Energy (US DOE) under contract no. DE-AC04-76DP00789.

The principal reference on which this paper is based was developed using Quality Assurance Level II controls. The synopsis documented in this paper was prepared using Quality Assurance Level NQ.

focal depth, maximum magnitude, fault width, activity rate, b-value, slip rate vs fault length relation, and fault length vs magnitude relation. The parameter variations were assigned weights, and all possible combinations were considered using a logic tree. A set of more than 60,000 ground acceleration hazard curves was generated and used to construct the 5, 50, and 95 percent confidence levels shown in Figure 2.

2.2 Ground Rupture Hazard

If all fault ruptures occur on known faults, the site rupture hazard will be zero. But since the Yucca Mountain site is in a highly faulted area, the possibility that an unknown fault exists under the WHB should be considered. The evaluation of the ground rupture hazard at the site for unknown faults is a new problem. Therefore, a variety of methods were developed in this study.

The methods for determining the rupture hazard at the site are based on both the probability that there is a fault under the WHB and the probability that the fault is not detected by a trenching program. Six different methods were used to estimate the rupture hazard: Midway Valley Fault (MV), imbricate faults, subsidiary fault rupture, random faulting (moment rate), random faulting within a 10 km cross section (strain rate), and random faulting as a function of slip rate (self similarity). The details of each method are briefly described in SNL (1988).

As with the acceleration hazard, the uncertainty in the ground rupture hazard was estimated by varying significant model parameters. In all, over 4,000 ground rupture hazard curves were generated. The median ground rupture hazards from each of the six methods are shown in Figure 3.

The site characterization plan at Yucca Mountain includes an extensive trenching program. If no faults are discovered during the trenching program, there will be more confidence that a fault does not exist under the site. The rupture hazards will be modified to include this additional information.

The curve in Figure 4 shows a subjective estimate of the probability that a trenching program will detect faults having various amounts of cumulative vertical displacement over 100,000 years in MV (SNL, 1988). The probability estimates took into account the nature and degree of stratification in the Quaternary units and the age of the units that are expected to be encountered. The rupture hazard curves were then combined with the probability-of-detection curve to estimate the total rupture hazard after trenching (assuming that no faults are detected). The 5, 50, and 95 percent confidence levels for this set of rupture hazard curves are shown in Figure 5.

2.3 Conditional Acceleration Hazard

If ground rupture occurs under the site, there is an associated peak acceleration. This acceleration is computed by using zero distance in the selected attenuation relation. The 5, 50, and 95 percent confidence levels for the ground acceleration hazard associated with a vertical rupture greater than 1 cm are shown in Figure 6. A comparison of these hazards with the hazards independent of rupture (Figure 2) indicates that almost all of the ground acceleration hazard is a result of earthquakes on nearby faults and not a result of earthquakes that produce rupture under the WHB site.

3.0 FRAGILITIES OF THE WHB

3.1 Seismic Analysis and Design

The structural system of the WHB consists of shear walls and slabs ranging from 2.0 to ~ 5 ft in thickness (SNL, 1987). Seismic joints separate the building into structurally independent blocks. The shear walls of the central part of the WHB are shown in Figure 7. This is the largest and heaviest structure in the building and has been selected for evaluation in this study.

A dynamic analysis of the structure was performed, using the model shown in Figure 8, for ground acceleration with a peak value of 0.4 g. The response of the structure to a vertical fault rupture underneath was computed using a static analysis. Depending on the assumed location of the fault line, the building may either tilt or partially overhang its foundation following the fault rupture, as shown in Figure 9. These two configurations of the building were analyzed for the acceleration loading that accompanies the fault displacement.

The shear forces and torsional moments in each element of the model were distributed to the walls, taking into consideration the direction and location of each wall. Horizontal and vertical reinforcement of the walls were designed using the ACI-349 Code, 4,000 psi concrete, and 60 ksi rebar. In addition, the shear forces in the walls were scaled by the PGA ratio and wall reinforcements were determined for a range of DBEs from 0.2 g to 1.0 g. The minimum reinforcement required by the code controlled the design for DBE levels of 0.2 g and 0.4 g for most of the walls.

3.2 Postulated Damage States

Four hypothetical damage states were defined for the shear walls. Interstory drift of shear walls was used as the parameter to quantify the damage states. The percentage drifts for light, moderate, heavy, and total damage states are 0.1, 0.2, 0.4, and 0.7, respectively.

3.3 Fragility Evaluation

Seismic fragility of structural elements is defined as the conditional probability that the element will achieve a predefined limit state (Cover et al., 1985; ASCE, 1986). These probabilities are computed based on the safety margin, F, for any limit state expressed as

$$F = F_s F_\mu F_{RS}$$

where F_s is the strength factor, F_μ is the ductility factor, and F_{RS} is the response factor. These factors are assumed to be random variables with a lognormal distribution and represent the effect of several parameters.

The strength factor is the ratio of the strength available to resist seismic loads to the design seismic loads (also referred to as the demand force). The ductility factor accounts for the inelastic energy absorption capacity of the structure. It is expressed in terms of the ductility ratio and the damping ratio. For the shear walls in the WHB, ductility ratios corresponding to the damage states were determined by taking the ratio of the story drifts to the assumed yield point drift of 0.15 percent. The response factor accounts for the conservatism and approximations in the methods of analysis used to determine the demand forces.

Composite fragility curves and fragility curves with confidence intervals were computed for the shear walls of WHB for all four damage states and for five design levels. Figures 10 and 11 are examples of the composite fragility curves. They demonstrate the relationship between the probabilities of exceeding a damage state as a function of the PGA and the reduction in the probabilities as the DBE level is increased. Figures 12 and 13 show the changes in the failure probabilities as the confidence level varies from 5 to 95 percent. All of these fragility curves are for the case of a ground acceleration without a fault rupture under the building. A sample of the fragility curves for a fault condition under the WHB is given in Figure 14, which corresponds to a vertical acceleration loading on the building together with 10 cm of vertical fault displacement.

4.0 DAMAGE PROBABILITIES

Seismic hazard curves and the fragility curves were convolved to obtain overall damage probabilities for all the design levels considered. Figure 15 shows the median estimate of these probabilities for four damage states. These probabilities are less than 10^{-6} for design levels as low as 0.2 g and for any damage state. The probability of exceeding a moderate damage state is 1.7×10^{-8} and 5×10^{-10} for the 0.2 g and 1.0 g designs, respectively. Figure 16 shows the damage probabilities with confidence intervals. The probabilities with a 95 percent confidence level may be 2 to 4 orders of magnitude larger than the median estimates. The contribution of the fault displacement to these probabilities is insignificant. This is mainly due to the very low probability of a fault rupture under the building and the low hazard values for the accompanying acceleration.

5.0 CONCLUSION

The computed damage probabilities for the WHB are very low for all the design levels considered. Therefore, the WHB poses a very low seismically induced risk even at seismic design levels as low as 0.2 g.

6.0 REFERENCES

ASCE (American Society of Civil Engineers), 1986. "Uncertainty and Conservatism in the Seismic Analysis and Design of Nuclear Facilities," New York, NY.

Cover, L. E., M. P. Bohn, R. D. Campbell, and D. A. Wesley, 1985. Handbook of Nuclear Power Plant Seismic Fragilities, Seismic Safety Margins Research Program, NUREG/CR-3558, Lawrence Livermore National Laboratory, Livermore, CA.

McGuire, R. K., 1976. "FORTRAN Computer Program for Seismic Risk Analysis", USGS-OFR-76-76, U.S. Geological Survey, Denver, CO.

McGuire, R. K., 1978. "FRISK: Computer Program for Seismic Risk using Faults as Earthquake Sources," USGS-OFR-78-1007, U.S. Geological Survey, Denver, CO.

SNL (Sandia National Laboratories), 1987. Compiled by H. R. MacDougall, L. W. Scully, and J. R. Tillerson, "Site Characterization Plan Conceptual Design Report," SAND84-2641, Albuquerque, NM.

SNL (Sandia National Laboratories), 1988. "Preliminary Seismic Design Cost-Benefit Assessment of the Tuff Repository Waste Handling Facilities," SAND88-1600, C. V. Subramanian et al., Albuquerque, NM.

URS/Blume, 1987. "Technical Basis and Parametric Study of Ground Motion and Surface Rupture Hazard Evaluation of Yucca Mountain, Nevada," SAND86-7013, Sandia National Laboratories, Albuquerque, NM.

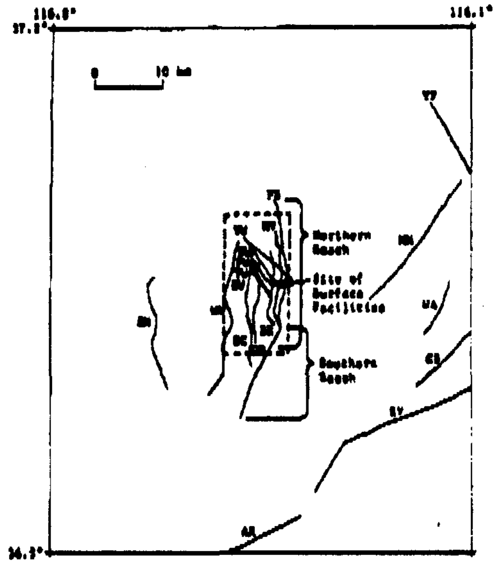

Figure 1. Active Fault Map of the Yucca Mountain Region (from URS/Blume, 1987)

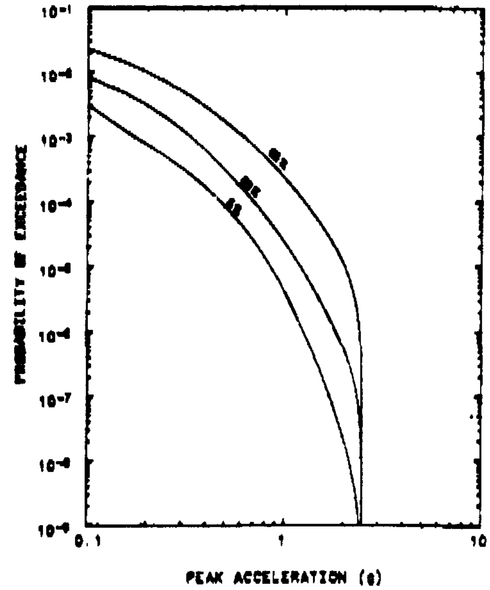

Figure 2. Horizontal Ground Acceleration Hazards for the WHB

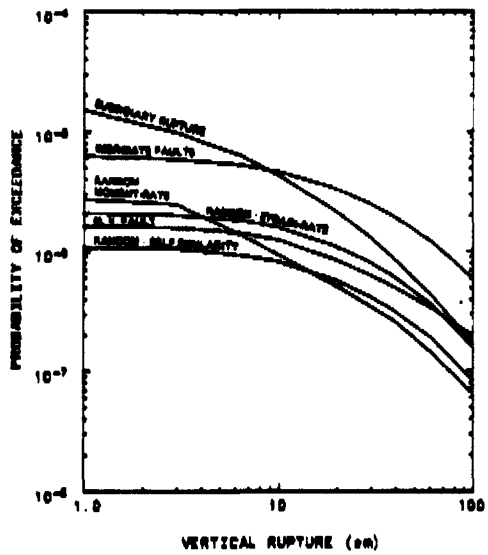

Figure 3. Median Rupture Hazards Before Trenching from the Six Methods

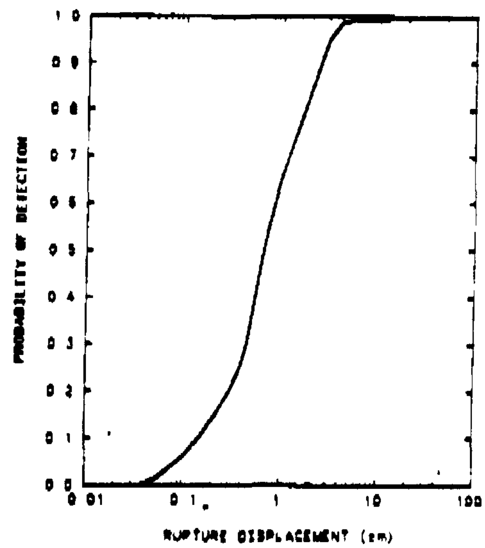

Figure 4. Assumed Probability That Faulting Will Be Detected by Trenching at Yucca Mountain

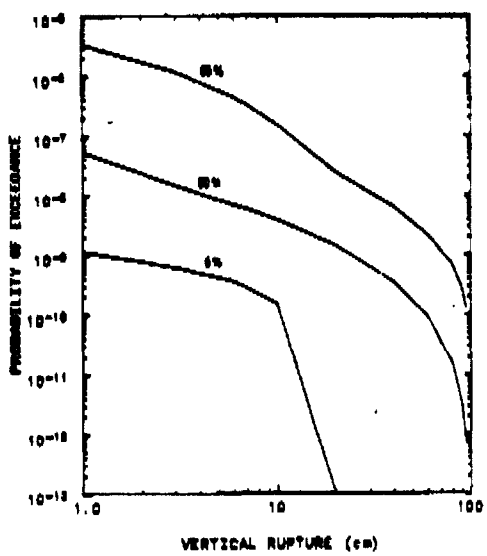

Figure 5. Ground Rupture Hazard for the WHB

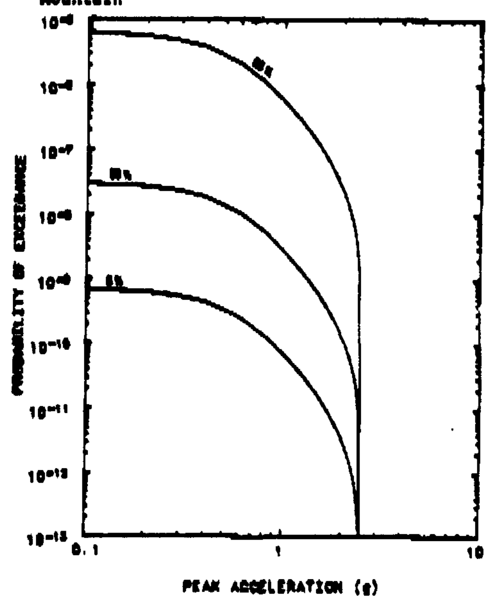

Figure 6. Horizontal Ground Acceleration Hazards Associated with Vertical Rupture Greater Than 1 cm

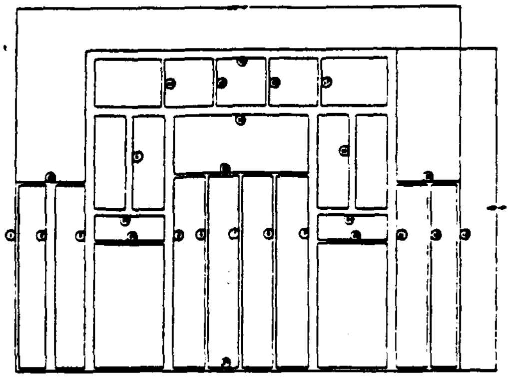

Figure 7. Shear Walls of the Central Part of the WHB at the First Floor (Elevation -25 ft to Grade)

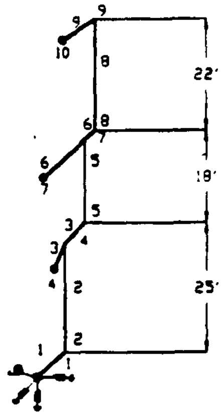

Figure 8. Seismic Model of the WHB

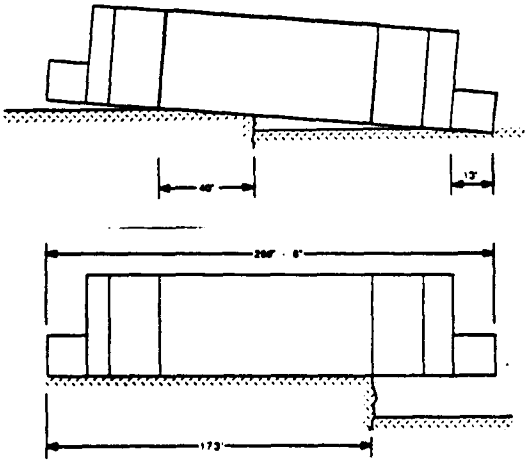

Figure 9. Tilted and Cantilevered Responses of the WHB to a Fault Rupture

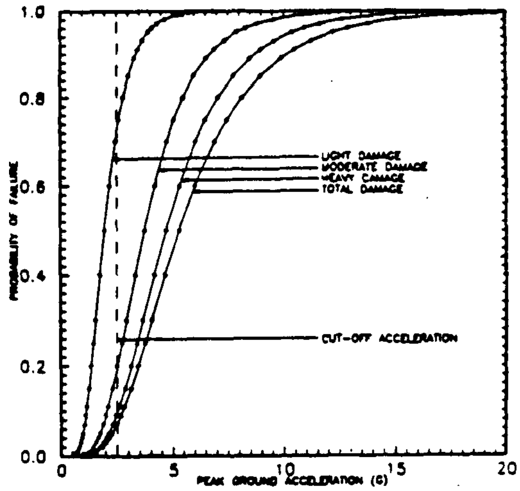

Figure 10. Composite Fragility Curves for the Average Wall, 0.4 g Design

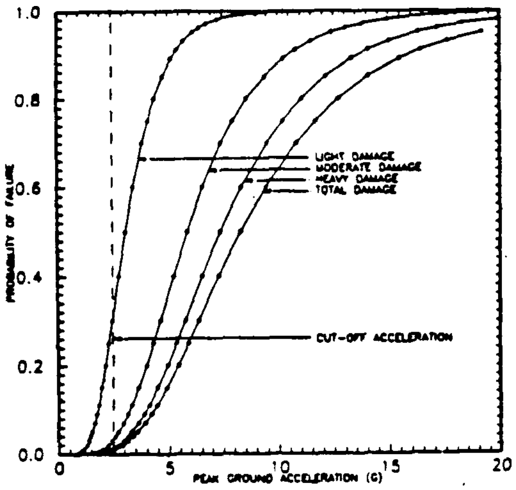

Figure 11. Composite Fragility Curves for the Average Wall, 1.0 g Design

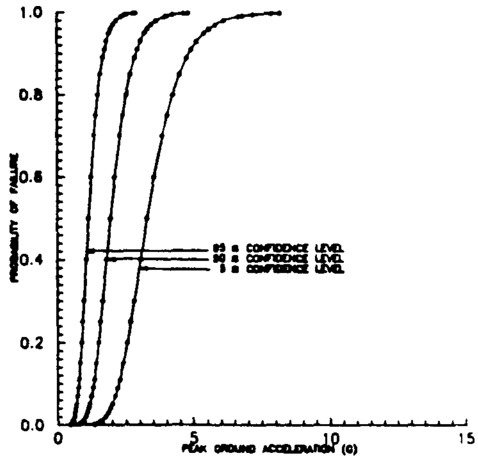

Figure 12. Fragility Curves with Confidence Intervals for the Light Damage State of the 0.2 g and 0.4 g Designs

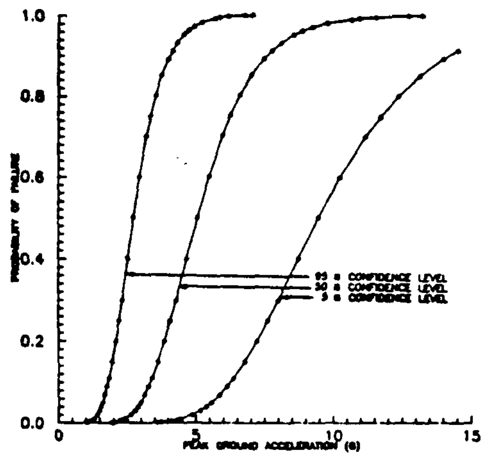

Figure 13. Fragility Curves with Confidence Intervals for the Total Damage State of the 0.2 g and 0.4 g Designs

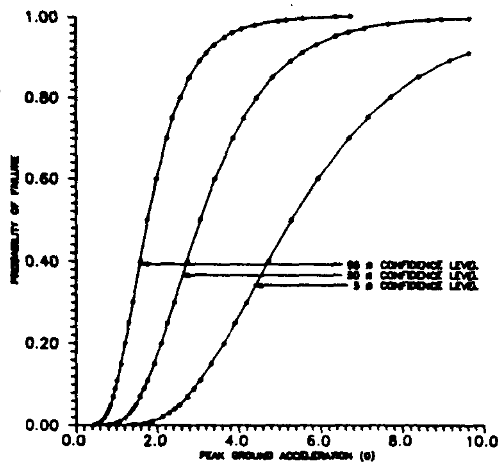

Figure 14. Fragility Curves with Confidence Intervals for the Case with a Fault Rupture Under the WHB for the Total Damage State of the 0.4 g Design

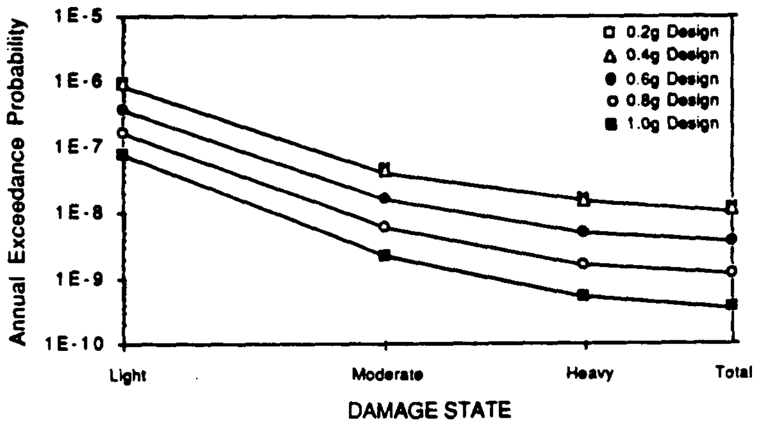

Figure 15. Median Estimate of Damage Probabilities of the WHB

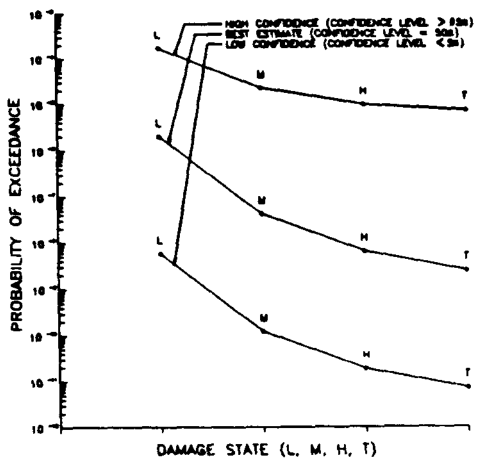

Figure 16. Damage Probability with Confidence Intervals for the 0.2 g and 0.4 g Designs

APPENDIX

Candidate Information
for the
Reference Information Base

Figure 1. Fault Map of the Yucca Mountain
Region (from URS/Blume, 1987)
is Candidate Information for the RIB

Candidate Information
for the
Site & Engineering Properties Data Base

This report contains no candidate information for the Site and Engineering Properties Data Base.